The Astronomical Journal, 147:38 (10pp), 2014 February doi:10.1088/0004-6256/147/2/38

CHROMOSPHERIC ACTIVITY AND ROTATIONAL MODULATION ON THE YOUNG, SINGLE K2 DWARF LQ Hya

Dong-tao Cao[1,2] and Sheng-hong Gu[1,2]
[1] Yunnan Observatories, Chinese Academy of Sciences, Kunming 650011, China; shenghonggu@ynao.ac.cn
[2] Key Laboratory for the Structure and Evolution of Celestial Objects, Chinese Academy of Sciences, Kunming 650011, China
Received 2013 August 26; accepted 2013 November 18; published 2014 January 9

ABSTRACT

High-resolution echelle spectra of LQ Hya, obtained during several observing runs from 2006 to 2012, have been analyzed to study its chromospheric activity. Using the spectral subtraction technique, we derived information about chromospheric activity of LQ Hya from several optical chromospheric activity indicators (including the H_β, He I D_3, Na I D_1, D_2, H_α, and Ca II infrared triplet (IRT) lines). No optical flares were found during our observations. The equivalent widths (EWs) of the excess emissions in the chromospheric activity lines have been measured. The ratios of EW_{8542}/EW_{8498} are generally small, which indicates that the Ca II IRT emission arises from plage-like regions, while the $E_{H\alpha}/E_{H\beta}$ values suggest that the emission of the Balmer lines is due to both plage and prominence structures for the observations in 2012. We find that clear rotational modulation of chromospheric emission exists, which suggests the presence and change of chromospheric active regions over the surface of LQ Hya. Moreover, the active regions were associated with the photospheric spots in spatial structure.

Key words: stars: activity – stars: chromospheres – stars: individual (LQ Hya) – stars: rotation

Online-only material: color figures

1. INTRODUCTION

LQ Hya (HD 82558) is a rapidly rotating, single K2 dwarf, classified as a BY Dra type variable star by Fekel et al. (1986b), with a rotation period of about 1.60066 days (Kővári et al. 2004). It is accepted to have just arrived on the zero-age main sequence and also shows extreme magnetic activity (Fekel et al. 1986a); therefore, LQ Hya has attracted much attention as a young solar analog.

LQ Hya exhibits strong chromospheric activity, as demonstrated by strong H_α emission above the continuum or sometimes completely filled-in H_α absorption (Fekel et al. 1986b; Vilhu et al. 1991; Strassmeier et al. 1993; Alekseev & Kozlova 2002; Frasca et al. 2008b), Ca II H and K (Strassmeier et al. 1990), and Ca II λ8498 and λ8542 core emission (Strassmeier et al. 1993; Basri & Marcy 1994). Also, strong flares on LQ Hya were detected in the X-ray (Covino et al. 2001), UV (Ambruster & Fekel 1990; Montes et al. 1999), and optical observations (Montes et al. 1999).

Photospheric spot activity has also been extensively studied by many authors with photometric investigations (Jetsu 1993; Strassmeier et al. 1993; Alekseev & Kozlova 2002; Berdyugina et al. 2002; Kővári et al. 2004; Lehtinen et al. 2012) and the Doppler imaging technique (Strassmeier et al. 1993; Rice & Strassmeier 1998; Kővári et al. 2004). Surface magnetic field patterns have also been presented by Donati (1999) and Donati et al. (2003) using Zeeman Doppler imaging.

In the present work, based on high-resolution spectra of LQ Hya obtained during several observing runs from 2006 to 2012, we aim at analyzing its chromospheric activity indicators and investigating chromospheric activity regions on the LQ Hya surface. Several activity indicators formed at different atmospheric levels are analyzed here, which include the H_α, H_β, Na I D_1, D_2, He I D_3, and Ca II infrared triplet (IRT) lines. Details of the observations and data reduction are given in Section 2, and the procedure of the spectral analysis is described in Section 3. In Section 4, the behavior of chromospheric activity indicators and the variation of chromospheric activity are discussed. Finally, we draw the conclusions of our study in Section 5.

2. OBSERVATIONS AND DATA REDUCTION

Spectroscopic observations of LQ Hya were performed during several observing seasons from 2006 to 2012. The observations were carried out with the 2.16 m telescope at the Xinglong station of the National Astronomical Observatories in China. The Coudé echelle spectrograph with a resolving power of about 37,000 and a 1024 × 1024 pixel Tektronix CCD detector were used during the observations in 2006 November 28–December 11, 2007 December 25, and 2008 November 11–17. The reciprocal dispersions are 0.079 Å pixel^{-1} for the Na I D_1, D_2, and He I D_3 spectral regions, 0.089 Å pixel^{-1} for the H_α spectral region, 0.114 Å pixel^{-1} for the Ca II λ8498 spectral region, 0.116 Å pixel^{-1} for the Ca II λ8542 spectral region, and 0.117 Å pixel^{-1} for the Ca II λ8662 spectral region. Correspondingly, the spectral resolutions in the same spectral regions determined as the FWHM of the arc comparison lines are 0.154, 0.167, 0.211, 0.219, and 0.228 Å, respectively.

On 2010 December 17, 18, and 20, and 2011 February 15 and 17, the spectroscopic observations of LQ Hya were made by using the Coudé echelle spectrograph with a 2048 × 2048 pixel EEV CCD detector, which suffers the heavily interferometric fringes in the near infrared wavelength region. The reciprocal dispersions are 0.045 Å pixel^{-1} for the Na I D_1, D_2, and He I D_3 spectral regions, 0.050 Å pixel^{-1} for the H_α spectral region, and the corresponding spectral resolutions are 0.140 and 0.156 Å, respectively.

On 2012 February 10–12, the observations were made by means of a new high-resolution fiber-fed echelle spectrograph with a spectral resolution of about 48,000 and a 4096 × 4096 pixel CCD detector. The reciprocal dispersions are 0.021 Å pixel^{-1} for the H_β spectral region, 0.025 Å pixel^{-1} for the Na I D_1, D_2, and He I D_3 spectral regions, 0.028 Å pixel^{-1} for the H_α spectral region, 0.036 Å pixel^{-1} for the Ca II λ8498 spectral region, and 0.037 Å pixel^{-1} for the Ca II λ8542 and

Table 1
Log of LQ Hya Spectroscopic Observations

Date	HJD (2,450,000+)	Phase	Exp. Time (s)	Date	HJD (2,450,000+)	Phase	Exp. Time (s)
2006 Nov 28	4068.4022	0.5162	3600	2010 Dec 20	5551.2406	0.9103	4500
2006 Nov 29	4069.4011	0.1402	3600	2010 Dec 20	5551.2948	0.9442	4500
2006 Dec 1	4071.3774	0.3749	3600	2010 Dec 20	5551.3487	0.9779	4500
2006 Dec 6	4076.3327	0.4707	3600	2010 Dec 20	5551.4083	0.0151	5400
2006 Dec 6	4076.3987	0.5119	3600	2011 Feb 15	5608.0938	0.4290	3600
2006 Dec 8	4078.3467	0.7289	3600	2011 Feb 15	5608.1370	0.4560	3600
2006 Dec 9	4079.3771	0.3726	3600	2011 Feb 15	5608.1746	0.4795	2700
2006 Dec 10	4080.3495	0.9802	3600	2011 Feb 15	5608.2077	0.5002	2700
2006 Dec 10	4080.4175	0.0226	3300	2011 Feb 15	5608.2455	0.5238	3600
2006 Dec 11	4081.3426	0.6006	3600	2011 Feb 15	5608.2884	0.5506	3600
2006 Dec 11	4081.3846	0.6268	3600	2011 Feb 17	5610.0875	0.6746	3600
2007 Dec 25	4460.2497	0.3205	1800	2011 Feb 17	5610.1305	0.7014	3600
2007 Dec 25	4460.3949	0.4112	2400	2011 Feb 17	5610.1679	0.7248	2700
2008 Nov 11	4782.3692	0.5626	3600	2011 Feb 17	5610.2051	0.7480	3600
2008 Nov 13	4784.3439	0.7963	2400	2011 Feb 17	5610.2481	0.7749	3600
2008 Nov 13	4784.3723	0.8141	3600	2011 Feb 17	5610.2908	0.8016	3600
2008 Nov 14	4785.3627	0.4328	2400	2012 Feb 10	5968.1344	0.3622	3600
2008 Nov 14	4785.3911	0.4506	2400	2012 Feb 10	5968.1846	0.3935	3600
2008 Nov 16	4787.3621	0.6819	3600	2012 Feb 10	5968.2348	0.4249	3600
2008 Nov 17	4788.3536	0.3013	3600	2012 Feb 10	5968.2852	0.4563	3600
2010 Dec 17	5548.2407	0.0362	3600	2012 Feb 10	5968.3354	0.4878	3600
2010 Dec 17	5548.2836	0.0629	3600	2012 Feb 11	5969.0997	0.9652	3600
2010 Dec 17	5548.3267	0.0899	3600	2012 Feb 11	5969.1639	0.0053	5400
2010 Dec 17	5548.3695	0.1166	3600	2012 Feb 11	5969.2406	0.0532	5400
2010 Dec 17	5548.4124	0.1434	3600	2012 Feb 11	5969.3187	0.1020	5400
2010 Dec 18	5549.2350	0.6573	4500	2012 Feb 12	5970.2039	0.6550	3600
2010 Dec 18	5549.2944	0.6945	5400	2012 Feb 12	5970.2723	0.6978	6740

Ca II λ8662 spectral regions, which yield relative spectral resolutions of 0.102–0.185 Å.

In Table 1, we give the observing log, which includes the observing date, heliocentric Julian date (HJD), rotational phase, and exposure time. The rotational phases were derived with the ephemeris:

$$\mathrm{HJD} = 2{,}448{,}270.0 + 1.600656 \times E \quad (1)$$

from Frasca et al. (2008b).

The spectrum reduction was performed with the IRAF[3] package following the standard reduction procedures. The wavelength calibration was obtained using the spectra of a Th–Ar lamp taken at the beginning and end of each observing night. Finally, all spectra were normalized by a low-order polynomial fit to the observed continuum.

In Figures 1–3, we display the normalized Ca II λ8662, Ca II λ8542, Ca II λ8498, H_α, Na I D_1, D_2, He I D_3, and H_β line profiles of LQ Hya obtained during our observations. The rotational phase and observing date are marked in the first panel of each figure.

For some observations during which telluric lines in the chromospheric activity line regions were heavy, a spectrum of the rapidly rotating early-type star HR 7894 (B5IV; $v \sin i = 330$ km s^{-1}) was used as the telluric template. The telluric lines in the spectra of LQ Hya are eliminated by means of this template with an interactive procedure, as described by Gu et al. (2002) in detail.

[3] IRAF is distributed by the National Optical Astronomy Observatories, which is operated by the Association of Universities for Research in Astronomy (AURA), Inc., under cooperative agreement with the National Science Foundation.

3. SPECTRAL ANALYSIS

In order to obtain the chromospheric contribution, we apply a method usually called the spectral subtraction technique, which was described in detail by Barden (1985) and Montes et al. (1995). This technique, which has been widely and successfully used for chromospheric activity studies (Gunn & Doyle 1997; Gunn et al. 1997; Montes et al. 1995, 1997, 2000; Gu et al. 2002; Zhang & Gu 2008; Frasca et al. 2008a, 2008b, 2010; Biazzo et al. 2009), subtracts a synthesized spectrum constructed from a spectrum of a reference star with the same spectral type and luminosity class as the active one. The synthesized spectrum represents the contribution of the non-active state, and the subtraction between the observed and the synthesized spectra could provide the pure chromospheric emission caused by activity.

For our situation, we observed some stars with spectral types and luminosity classes similar to LQ Hya as candidate reference stars. By comparison, HR 222 (K2V) was found to be a better reference star for LQ Hya in 2006–2011 observing runs, but it was not observed in 2012. Another star, HD 3765 (K2V), was used as a reference to construct a synthesized spectrum for the 2012 observations. In the course of the analysis, by means of the program STARMOD (Barden 1985), the synthesized spectrum was constructed by rotationally broadening the reference spectrum to $v \sin i = 28$ km s^{-1} (Kővári et al. 2004) and shifting along the radial-velocity axis, and consequently the subtracted spectra were calculated. Examples of spectral subtraction in the different spectral regions are displayed in Figure 4.

The equivalent widths (EWs) of the excess emission in the different chromospheric diagnostics were measured in the subtracted spectra using the IRAF/SPLOT task. We determined the EWs by integrating over the emission profile in the subtracted spectra, and additionally measured them using a Gaussian

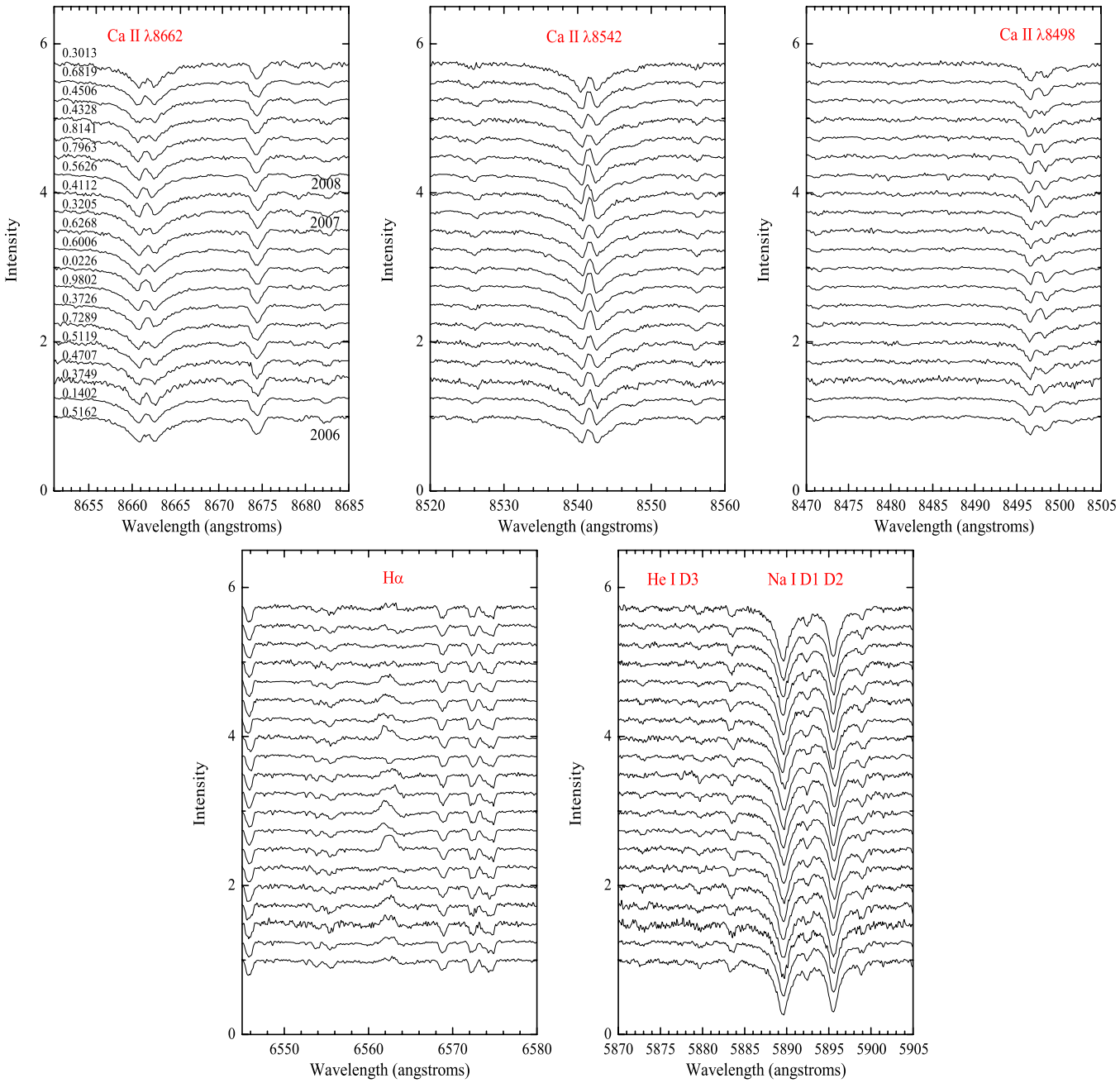

Figure 1. Ca II λ8662, Ca II λ8542, Ca II λ8498, H_α, He I D_3, and Na I D_1, D_2 lines of LQ Hya observed in 2006–2008 and shifted arbitrarily.
(A color version of this figure is available in the online journal.)

function fit. (For some profiles, we needed several Gaussian profiles to fit them.) The final EWs were derived by taking the mean values of the two methods, and are listed in Table 2 along with their errors. The errors for the measured EWs were estimated using the difference between the measurements of the two methods.

In Table 2 we also give the ratio of excess emission EW_{8542}/EW_{8498} for the 2006–2008 and 2012 observing runs, and calculate the ratio of excess emission $E_{H\alpha}/E_{H\beta}$ with the correction for the observations obtained in the 2012 run,

$$\frac{E_{H\alpha}}{E_{H\beta}} = \frac{EW(H_\alpha)}{EW(H_\beta)} * 0.2444 * 2.512^{(B-R)}, \quad (2)$$

given by Hall & Ramsey (1992), where the first term on the right side is the ratio of excess emission EWs, the second term (0.2444) is the ratio of the absolute flux density at the H_α and H_β lines, and the last term takes into account the color difference in the components. The color index $B-R = 1.66$ (Alekseev & Kozlova 2002) was used for the calculation.

4. DISCUSSION

4.1. Chromospheric Activity Indicators

Chromospheric activity lines that formed at different atmospheric heights, such as the H_α, H_β (formed in the middle chromosphere), Na I D_1, D_2 (upper photosphere and lower chromosphere), He I D_3 (upper chromosphere), and Ca II IRT (lower chromosphere) lines were observed for LQ Hya during our observations. These lines have been proven to be very important and useful chromospheric activity indicators in the

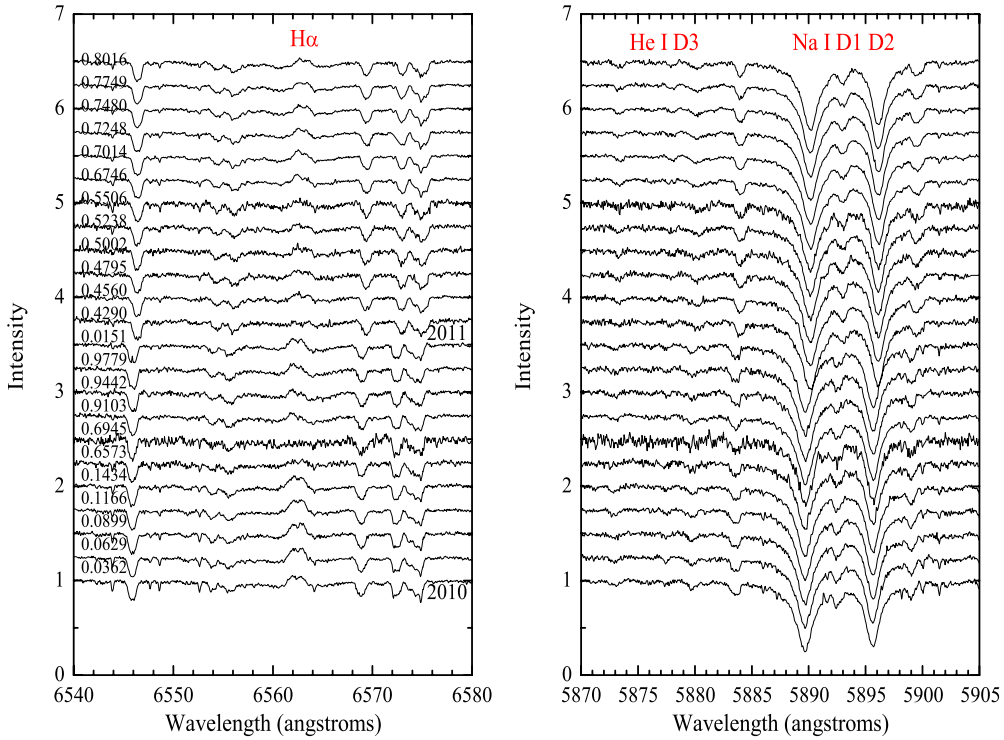

Figure 2. H_α, He I D_3, and Na I D_1, D_2 lines of LQ Hya derived in 2010–2011 and shifted arbitrarily.
(A color version of this figure is available in the online journal.)

optical spectral range from the region of temperature minimum to the upper chromosphere (Gunn & Doyle 1997; Gunn et al. 1997; Montes et al. 1995, 1997, 2000), which can help us to investigate information about the chromospheric structure.

4.1.1. The H_α and H_β Lines

The H_α line usually shows emission above the continuum in very active stars, while appears as a filled-in absorption profile in less active ones (Montes et al. 1997, 2000). In all the spectra of LQ Hya, we can see that the H_α line is a strongly variable feature, exhibiting variation from a completely filled-in absorption to a strong emission above the continuum (see Figures 1–3), which demonstrates that LQ Hya is a very active star and shows possible rotational modulation of chromospheric activity. Also, the H_α emission profiles show double peaks with central reversal and mostly asymmetry, as observed by Strassmeier et al. (1993), Alekseev & Kozlova (2002), and Frasca et al. (2008b). Strassmeier et al. (1993) attributed this variable H_α emission asymmetry to the presence of chromospheric velocity fields and rotational modulation of bright plages. In addition, Frasca et al. (2008b) concluded that the rotational modulation of profile asymmetry is associated with the presence of plage-like regions on the surface of LQ Hya.

Another Balmer line, H_β, was also available in our spectra observed in the 2012 run, and appears always in absorption (see Figure 3). After applying the spectral subtraction technique, chromospheric emission obviously presents in the subtracted H_β spectral region (see Figure 4), and is much smaller than the H_α line. For LQ Hya, the H_β line changed from mostly filled-in absorption to a strong and broad emission profile during an optical flare event, reported by Montes et al. (1999).

The $E_{H\alpha}/E_{H\beta}$ values have been used usually as a diagnostic for discriminating between the presence of prominences and plages on the stellar surface. Buzasi (1989) developed an NLTE radiative transfer model and concluded that low ratios (∼1–2) can be achieved both in plages and prominences viewed against the disk, but high values (∼3–15) can only be achieved in prominence-like structures viewed off the stellar limb. Typical observational values are ∼10 in solar prominences seen at the limb (Landman & Mongillo 1979), and ∼1–2 in solar plages (Chester 1991). Therefore, the values (∼2.5–3.5) we found in LQ Hya during our 2012 observing run reveal that the emission in the Balmer lines is mainly due to plage regions, consistent with the result inferred from the EW_{8542}/EW_{8498} ratios, and extended prominence-like structures may play a role sometimes.

Moreover, in order to investigate the relation between the $E_{H\alpha}/E_{H\beta}$ values and chromospheric activity variations, we plot the EWs of chromospheric H_α and H_β lines and the ratios as a function of the rational phase in Figure 5. We find that the $E_{H\alpha}/E_{H\beta}$ ratios are much smaller during the phase interval of high activity (phases 0.6550–0.6978) and decrease with the increase of chromospheric activity, which indicates that plage emission dominates the variation of chromospheric activity in the H_α and H_β lines.

4.1.2. The Ca II IRT Lines

The Ca II IRT lines show emission cores in all spectra during our observations, and the emission is the strongest for the λ8542 line, a little weaker for the λ8662 line, and the weakest for the λ8498 line (see Figure 4). Similar features in the Ca II IRT lines have also been found in several other chromospheric activity stars (Gu et al. 2002; Biazzo et al. 2009; Montes et al. 2000). This self-reversal core emission could be ascribed to plages, and the increased emission results from the higher temperature and higher electron densities at a given line optical depth produced

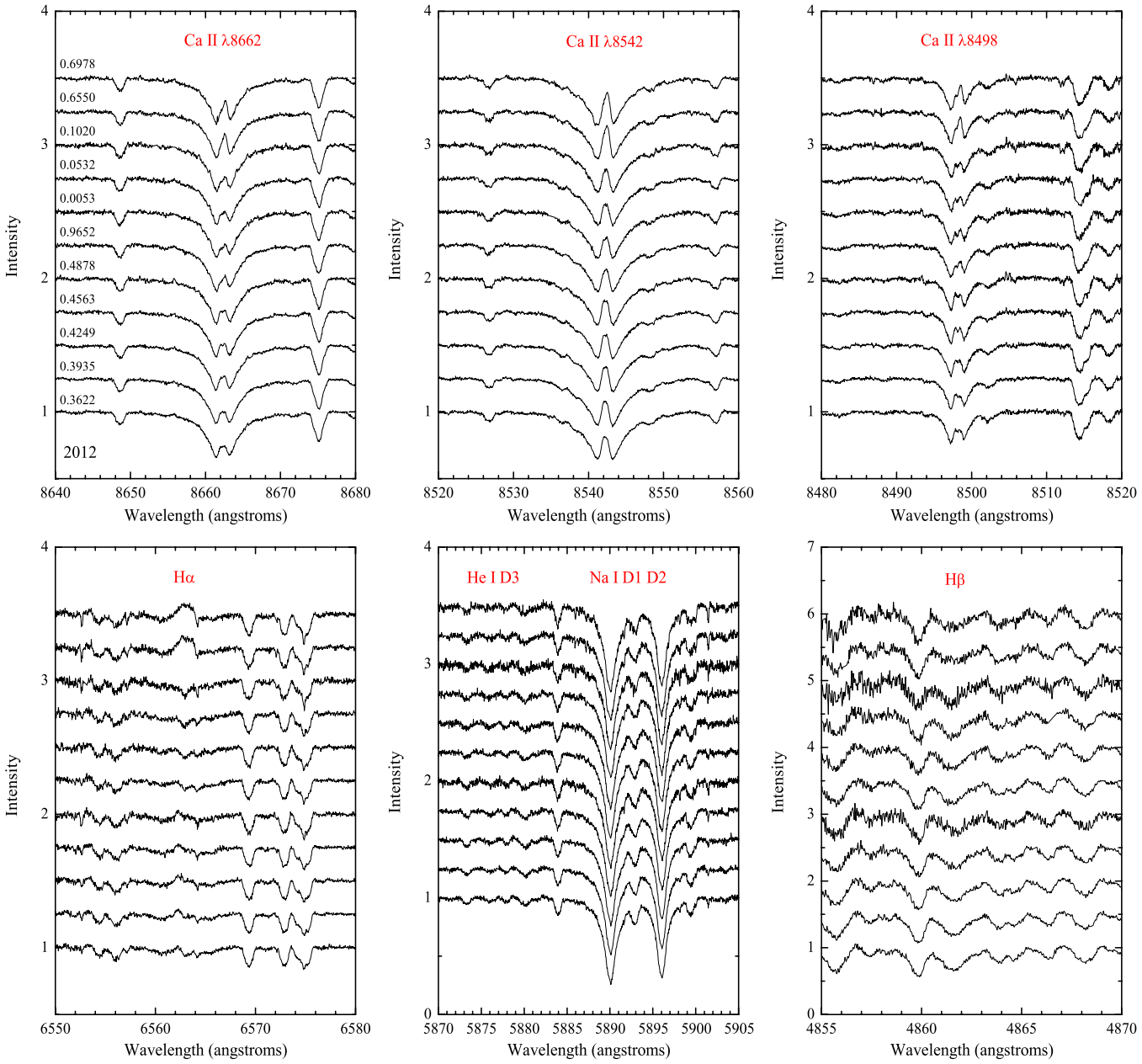

Figure 3. Ca II λ8662, Ca II λ8542, Ca II λ8498, H_α, He I D_3, Na I D_1, D_2, and H_β line profiles of LQ Hya, obtained in the 2012 run and shifted arbitrarily. (A color version of this figure is available in the online journal.)

by the steeper temperature gradient (Shine & Linsky 1972, 1974). Moreover, asymmetry of the chromospheric emission profile with a central reversal has been detected for the Ca II IRT lines at some phases (see Figures 1 and 3). This asymmetric situation has also been found by Strassmeier et al. (1993) for LQ Hya and by Montes et al. (2000) for several other active stars. A similar feature was mostly observed in the Sun's Ca II K line (Zirin 1988).

Moreover, the ratio of excess emission EW, EW_{8542}/EW_{8498} is also an indicator of the type of chromospheric structure that produces the observed Ca II IRT emission. In solar prominences, typical values are ~ 9 (Chester 1991). For LQ Hya, however, the ratios are found in the range of 1–2 (see Table 2), approximating the values in solar plages ($\sim$1.5–3; Chester 1991), which indicates that Ca II IRT emission arises predominantly from plage-like regions. These low values are also presented in several other chromospheric active stars (Montes et al. 2000; Gu et al. 2002; López-Santiago et al. 2003; Zhang & Gu 2008; Gálvez et al. 2009; Frasca et al. 2010).

4.1.3. The Na I D_1, D_2 and He I D_3 Lines

The Na I D_1, D_2 lines are very sensitive to the effective temperature, so the slight difference in temperature between active and reference stars would produce significant changes in the wings of the Na I subtraction profiles (Montes et al. 1997). For our situation, the Na I D_1, D_2 lines are characterized by deep absorption (see Figures 1–3), and show weak excess emission in the subtracted spectra during the observations from 2006 to 2011 (see Figure 4). However, the synthesized Na I D_1, D_2 profiles mismatched the observational ones in our 2012 observing run, due to using a different reference star.

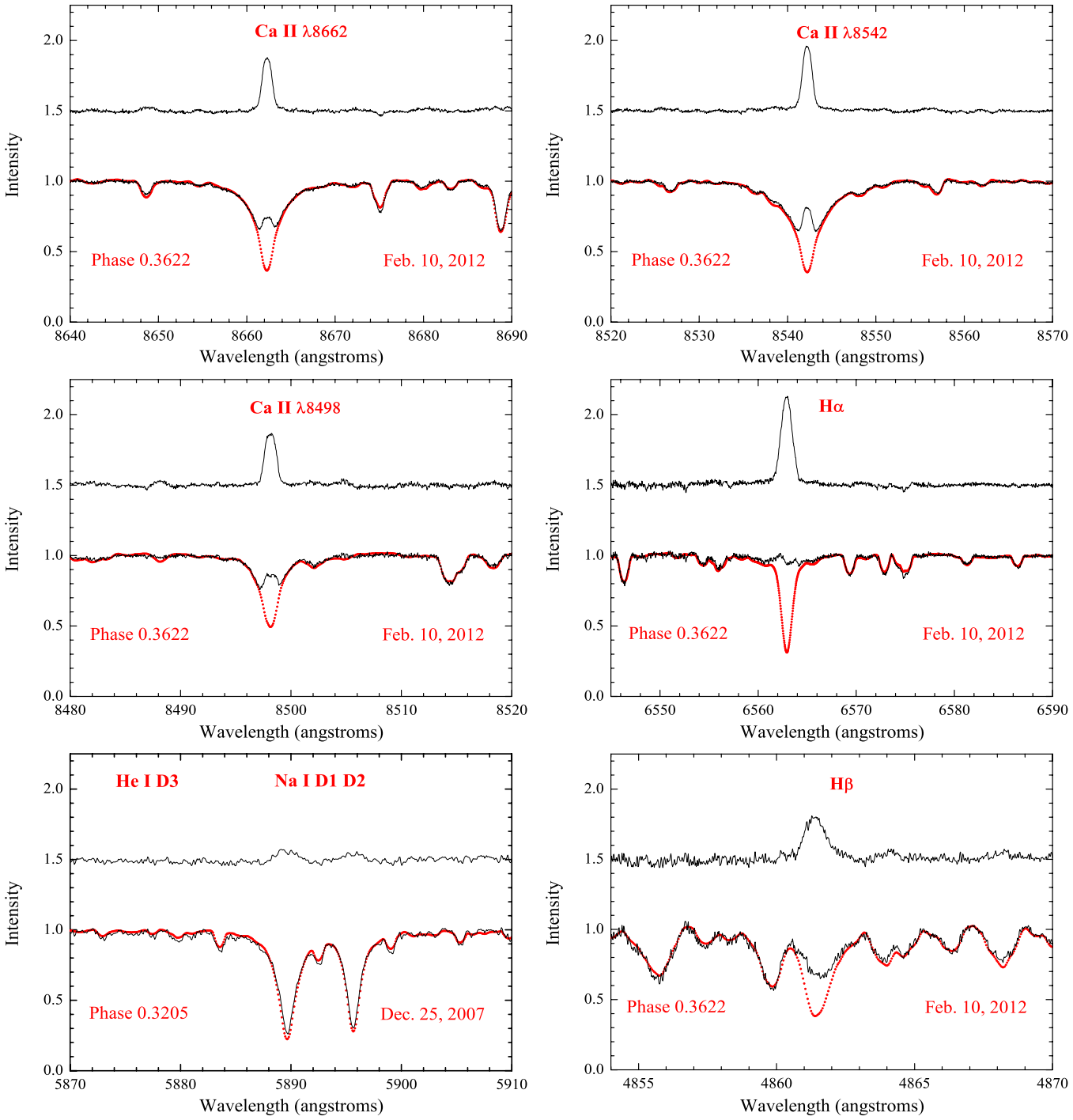

Figure 4. Examples of the observed, synthesized, and subtracted spectra for the Ca II IRT, H_α, and H_β line spectral regions observed in the 2012 observing run, and He I D_3 and Na I D_1, D_2 line spectral regions obtained in the 2007 observing run. For each panel, the dotted line represents the synthesized spectrum and the upper spectrum is the subtracted one, shifted for better display.

(A color version of this figure is available in the online journal.)

The behavior of the He I D_3 line is a good indicator of the activities of the Sun and late-type stars. Because it has a very high excitation level, it is a useful diagnostic of optical flares if this line is in emission (Zirin 1988; Montes et al. 1997, 1999). It has also been seen as an absorption feature attributed to plages (Huenemoerder 1986). Comparing with the synthesized spectrum, however, LQ Hya does not show any emission or absorption features in our observations (see Figure 4). It was the only time that an optical flare was found by Montes et al. (1999), through the He I D_3 line emission and simultaneous observations of other several frequently used chromospheric lines: H_α, H_β, Na I D_1, D_2, and Mg I b triplet lines.

4.2. Rotational Modulation of Chromospheric Activity

The variability of chromospheric emission with rotational phase indicates that the distribution of active regions is not uniform on the stellar surface, and can help us to derive the location of active regions. These chromospheric activity regions are similar to the solar plages, and have been found in many

Table 2
The Measurements for Excess Emissions of the Ca II IRT, H_α, and H_β Lines in the Subtracted Spectra

Phase	EW (Å)					$\frac{EW_{8542}}{EW_{8498}}$	$\frac{E_{H\alpha}}{E_{H\beta}}$
	Ca II λ8662	Ca II λ8542	Ca II λ8498	H_α	H_β		
			2006				
0.5162	0.445 ± 0.014	0.590 ± 0.006	0.389 ± 0.012	1.291 ± 0.023	···	1.55	···
0.1402	0.485 ± 0.020	0.618 ± 0.016	0.412 ± 0.026	1.323 ± 0.020	···	1.50	···
0.3749	0.474 ± 0.014	0.589 ± 0.006	0.390 ± 0.008	1.363 ± 0.021	···	1.51	···
0.4707	0.502 ± 0.012	0.651 ± 0.002	0.445 ± 0.004	1.448 ± 0.010	···	1.46	···
0.5119	0.499 ± 0.014	0.590 ± 0.010	0.399 ± 0.026	1.410 ± 0.025	···	1.48	···
0.7289	0.414 ± 0.026	0.591 ± 0.004	0.389 ± 0.026	1.165 ± 0.015	···	1.52	···
0.3726	0.531 ± 0.014	0.722 ± 0.008	0.473 ± 0.008	1.631 ± 0.025	···	1.53	···
0.9802	0.520 ± 0.012	0.745 ± 0.022	0.467 ± 0.016	1.342 ± 0.029	···	1.60	···
0.0226	0.555 ± 0.014	0.730 ± 0.002	0.483 ± 0.012	1.452 ± 0.033	···	1.51	···
0.6006	0.523 ± 0.014	0.629 ± 0.002	0.436 ± 0.004	1.405 ± 0.025	···	1.44	···
0.6268	0.483 ± 0.012	0.600 ± 0.012	0.398 ± 0.020	1.351 ± 0.019	···	1.51	···
			2007				
0.3205	0.541 ± 0.025	0.605 ± 0.040	0.419 ± 0.020	1.026 ± 0.020	···	1.44	···
0.4112	0.601 ± 0.020	0.693 ± 0.021	0.516 ± 0.011	1.440 ± 0.022	···	1.34	···
			2008				
0.5626	0.528 ± 0.022	0.591 ± 0.019	0.443 ± 0.023	1.214 ± 0.022	···	1.33	···
0.7963	0.529 ± 0.025	0.580 ± 0.021	0.471 ± 0.028	1.232 ± 0.026	···	1.23	···
0.8141	0.514 ± 0.026	0.572 ± 0.022	0.452 ± 0.027	1.239 ± 0.029	···	1.27	···
0.4328	0.499 ± 0.017	0.536 ± 0.026	0.394 ± 0.022	1.095 ± 0.035	···	1.36	···
0.4506	0.481 ± 0.028	0.535 ± 0.025	0.382 ± 0.016	1.057 ± 0.027	···	1.40	···
0.6819	0.512 ± 0.024	0.601 ± 0.022	0.433 ± 0.026	0.965 ± 0.028	···	1.39	···
0.3013	0.474 ± 0.029	0.526 ± 0.025	0.398 ± 0.022	1.150 ± 0.033	···	1.32	···
			2010				
0.0362	···	···	···	1.232 ± 0.019	···	···	···
0.0629	···	···	···	1.260 ± 0.027	···	···	···
0.0899	···	···	···	1.339 ± 0.035	···	···	···
0.1166	···	···	···	1.381 ± 0.025	···	···	···
0.1434	···	···	···	1.399 ± 0.029	···	···	···
0.6573	···	···	···	1.383 ± 0.022	···	···	···
0.6945	···	···	···	1.168 ± 0.032	···	···	···
0.9103	···	···	···	1.083 ± 0.045	···	···	···
0.9442	···	···	···	1.109 ± 0.020	···	···	···
0.9779	···	···	···	1.119 ± 0.025	···	···	···
0.0151	···	···	···	1.145 ± 0.022	···	···	···
			2011				
0.4290	···	···	···	1.152 ± 0.025	···	···	···
0.4560	···	···	···	1.206 ± 0.040	···	···	···
0.4795	···	···	···	1.203 ± 0.042	···	···	···
0.5002	···	···	···	1.183 ± 0.020	···	···	···
0.5238	···	···	···	1.186 ± 0.020	···	···	···
0.5506	···	···	···	1.189 ± 0.046	···	···	···
0.6746	···	···	···	1.206 ± 0.030	···	···	···
0.7014	···	···	···	1.216 ± 0.038	···	···	···
0.7248	···	···	···	1.205 ± 0.025	···	···	···
0.7480	···	···	···	1.161 ± 0.027	···	···	···
0.7749	···	···	···	1.182 ± 0.032	···	···	···
0.8016	···	···	···	1.157 ± 0.026	···	···	···
			2012				
0.3622	0.544 ± 0.013	0.690 ± 0.017	0.480 ± 0.014	0.925 ± 0.016	0.300 ± 0.016	1.44	3.48
0.3935	0.553 ± 0.014	0.705 ± 0.018	0.499 ± 0.018	1.010 ± 0.020	0.359 ± 0.022	1.41	3.17
0.4249	0.590 ± 0.015	0.729 ± 0.022	0.499 ± 0.010	1.036 ± 0.022	0.378 ± 0.016	1.46	3.09
0.4563	0.578 ± 0.015	0.724 ± 0.023	0.488 ± 0.008	0.979 ± 0.020	0.350 ± 0.018	1.48	3.15
0.4878	0.577 ± 0.015	0.733 ± 0.020	0.489 ± 0.006	0.982 ± 0.018	0.395 ± 0.026	1.50	2.80
0.9652	0.577 ± 0.017	0.699 ± 0.020	0.465 ± 0.010	0.904 ± 0.018	0.314 ± 0.012	1.50	3.25
0.0053	0.584 ± 0.020	0.693 ± 0.023	0.444 ± 0.008	0.893 ± 0.024	0.351 ± 0.022	1.56	2.87
0.0532	0.573 ± 0.019	0.689 ± 0.022	0.449 ± 0.010	0.860 ± 0.020	0.284 ± 0.010	1.53	3.42
0.1020	0.593 ± 0.020	0.685 ± 0.019	0.457 ± 0.014	0.823 ± 0.014	0.290 ± 0.004	1.50	3.20
0.6550	0.610 ± 0.014	0.761 ± 0.018	0.525 ± 0.002	1.116 ± 0.020	0.489 ± 0.032	1.45	2.57
0.6978	0.636 ± 0.017	0.773 ± 0.018	0.515 ± 0.004	1.099 ± 0.022	0.495 ± 0.030	1.50	2.50

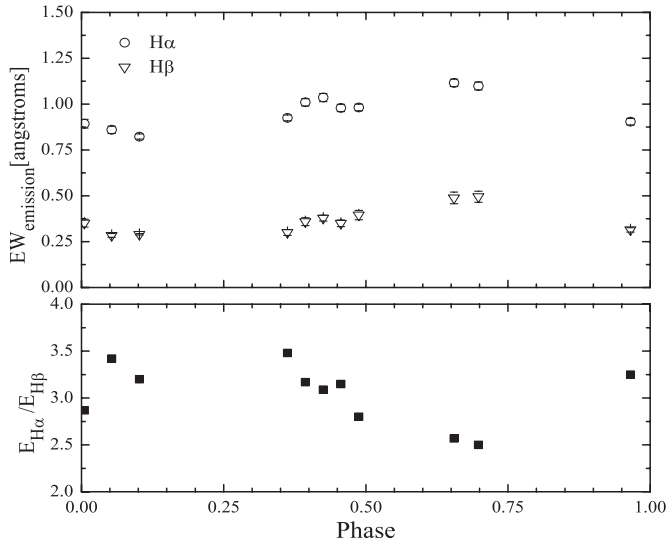

Figure 5. Comparison between the $E_{H\alpha}/E_{H\beta}$ ratios and chromospheric emission variations in H_α and H_β lines.

active stars by means of several chromospheric diagnostics (Gu et al. 2002; Frasca et al. 2008a, 2008b, 2010; Zhang & Gu 2008; Biazzo et al. 2009).

In order to analyze the possible rotational modulation of chromospheric activity of LQ Hya, the observations of each observing run were grouped together, respectively. We plot the EWs of Ca II IRT, H_α, and H_β excess emission profiles against rotational phase in Figure 6.

Although a slight scatter existed in the Ca II IRT and H_α excess emission EWs during the 2006 epoch, a detectable rotational modulation could still be found. Chromospheric emissions of two spectra at the same phase (0.37) obtained on different observing nights were obviously different, probably due to additional microflare features. From Figure 6, it is clear that the EWs of H_α and Ca II IRT excess emission profiles are correlated, and two active longitudes existed near rotational phases 0.0 and 0.5. However, observations obtained during the 2012 epoch reveal that one active longitude locates at about rotational phase 0.7 (see Figure 6), probably indicating a large plage-like region there.

For the observations obtained during the other observing runs, there was no good phase coverage. Although only two spectra were obtained in one observing night of 2007, at phase 0.32 and 0.41, the observations reveal extreme enhancement in chromospheric emission, which also indicated possible rotational modulation. A clear active longitude could be found near phase 0.15 in 2010.

There is a close spatial association between photospheric spots and chromospheric plages for most active stars; usually, the behavior of chromospheric activity lines is anti-correlated with the optical light curve, which indicates that plages are mainly concentrated in the regions above dark starspots (García-Alvarez et al. 2003; Frasca et al. 2008a, 2010; Biazzo et al. 2009). For LQ Hya, a close association between plages and spots has been reported by Strassmeier et al. (1993) and Frasca et al. (2008b). Photometric observations published by Lehtinen et al. (2012) for the mean epochs 2006.93, 2007.94, 2008.95, 2010.95, and 2011.13, were carried out at similar times with our spectroscopic observations in 2006–2011 observing runs, respectively. To make a comparison between chromospheric and photospheric activity for LQ Hya, we recalculate the rotational phases of our observations using their ephemeris and plot the EWs of the H_α excess emission against phase in Figure 7. By comparing the variation of the chromospheric emission with the light curves presented in Figure 2 of Lehtinen et al. (2012), clear anti-correlations are found: the EWs approach their maximum when LQ Hya becomes the faintest in the 2006 observing run, the chromospheric emission in two spectra of 2007 increases along with a decrease of the corresponding light curve, and the chromospheric active longitude is very close to a spot region in 2010. Moreover, active longitudes have been found using photometry and the Doppler imaging technique by several authors, Jetsu (1993), Strassmeier et al. (1993), Rice & Strassmeier (1998), Berdyugina et al. (2002), and Kővári et al. (2004), but there was not a stable pattern. Based on 24 yr photometry of LQ Hya from 1988 to 2011, Lehtinen et al. (2012) concluded that the active regions seem to be stable on timescales of up to six months, and, except for a few instances, no persistent active longitudes exist on timescales longer than 1 yr. Chromospheric activity variations derived in 2006 show that two active longitudes presented on the surface of LQ Hya, which resembles the results obtained by Berdyugina et al. (2002) through photometric observations spanning almost 20 yr. However, only one large plage-like region was found during 2012, and active longitudes presented over the surface of LQ Hya in other observing runs, suggesting that the chromospheric active regions were changing during 2006–2012.

Moreover, from Figure 6 it is found that the chromospheric activity level (especially for the H_α line) gradually decreased from 2006 to 2012, and it was anti-correlated with the long-term variations of the light curve found by Lehtinen et al. (2012), that the mean brightness of LQ Hya increased steadily from 2002 to the end of the observations (the year of 2011). The cyclic behavior over several years in the photospheric spot activity of LQ Hya has been reported based on light variations (Jetsu 1993; Berdyugina et al. 2002; Kővári et al. 2004). To infer its possible chromospheric activity cycle, we may require more frequent observations over several years in the future.

5. CONCLUSIONS

Based on the above analysis for our spectroscopic observations, we have obtained information about the chromospheric activity of LQ Hya with several different chromospheric activity indicators during 2006–2012.

Strong chromospheric emission in the H_α, H_β, and Ca II IRT lines confirms the strong magnetic activity of LQ Hya. No flares were detected during our observations. The ratios of EW_{8542}/EW_{8498} indicate that the Ca II IRT emission arises from plage-like regions, while the $E_{H\alpha}/E_{H\beta}$ values manifest that the emission of the Balmer lines is due to both plage and prominence structures for the observations in 2012, and plage emission dominates the variation of the chromospheric activity in the Balmer lines.

Rotational modulation of the chromospheric activity in the Ca II IRT, H_α, and H_β lines was found, which suggests the presence and change of the chromospheric active longitude over the surface of LQ Hya during our observations. Moreover, the chromospheric activity level gradually decreased from 2006 to 2012. By comparing with the light curve variations found by Lehtinen et al. (2012), a close spatial connection of photospheric and chromospheric active regions was detected for LQ Hya.

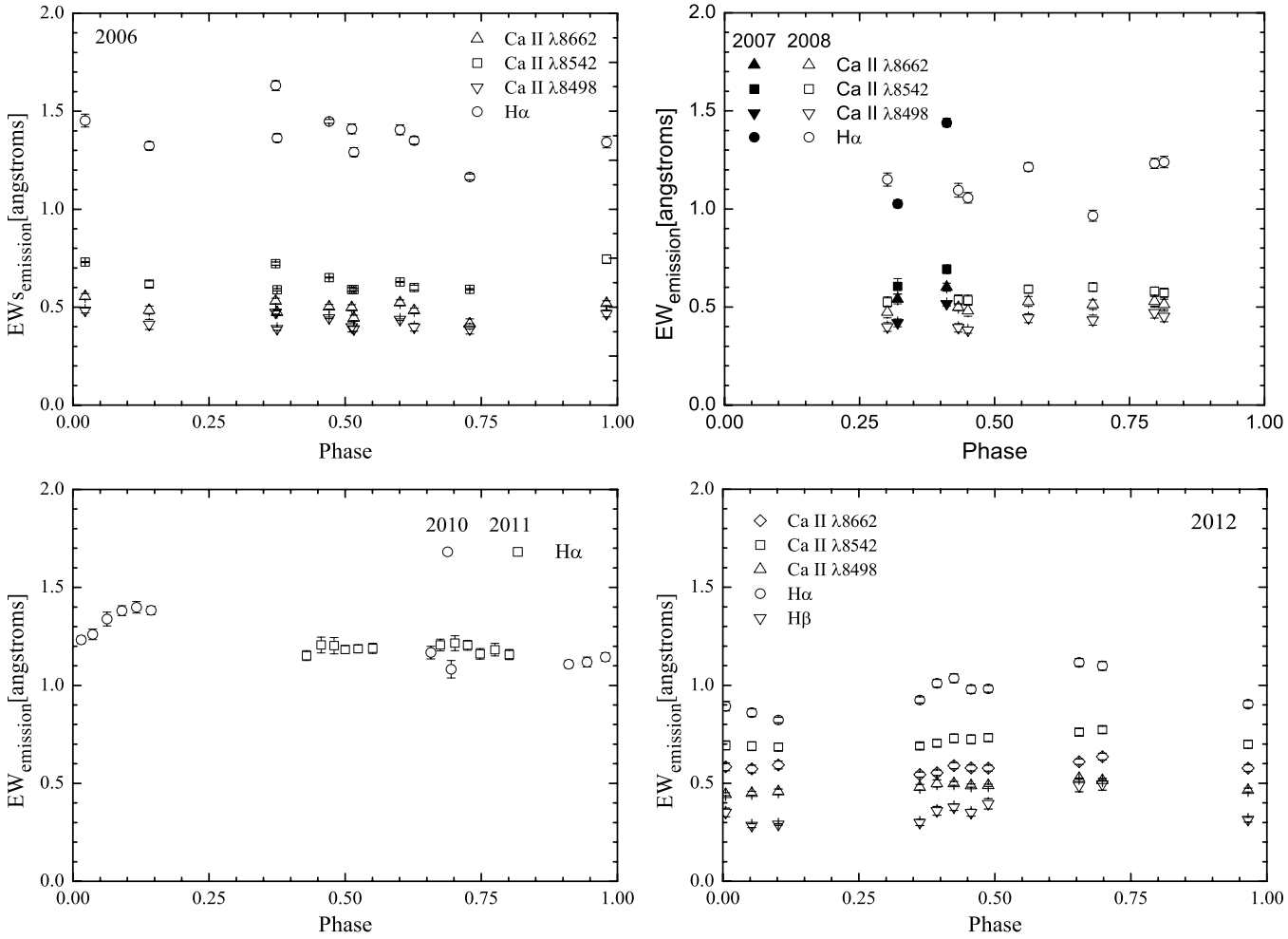

Figure 6. EWs of the excess emissions as a function of the rotational phase.

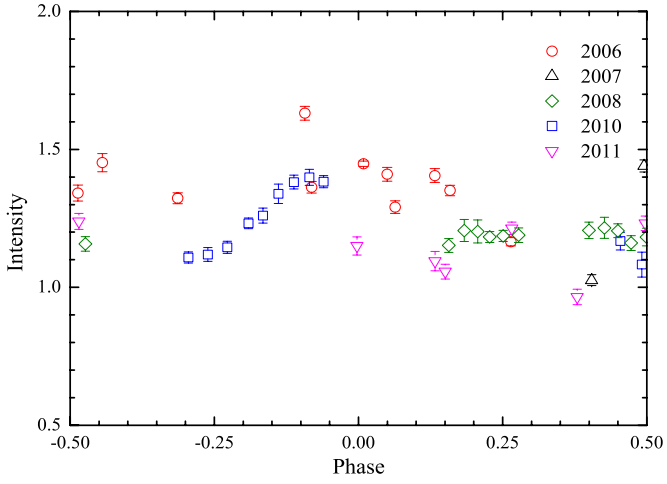

Figure 7. EWs of the excess emissions vs. the recalculated rotational phase for the H_α line in the 2006–2011 observing runs.

(A color version of this figure is available in the online journal.)

We are grateful to Dr. Montes for providing a copy of the STARMOD program. We thank the observing assistants of the 2.16 m telescope of Xinglong station of National Astronomical Observatories for their support during our observations. We also thank the anonymous referee for helpful comments and suggestions. This work is supported by the NSFC under grant Nos. 10373023, 10773027, and 11333006, and the Chinese Academy of Sciences through project KJCX2-YW-T24.

REFERENCES

Alekseev, I. Yu., & Kozlova, O. V. 2002, A&A, 396, 203
Ambruster, C., & Fekel, F. C. 1990, BAAS, 22, 857
Barden, S. C. 1985, ApJ, 295, 162
Basri, G., & Marcy, G. W. 1994, ApJ, 431, 844
Berdyugina, S. V., Pelt, J., & Tuominen, I. 2002, A&A, 394, 505
Biazzo, K., Frasca, A., Marilli, E., et al. 2009, A&A, 499, 579
Buzasi, D. L. 1989, PhD thesis, Pennsylvania State Univ.
Chester, M. M. 1991, PhD thesis, Pennsylvania State Univ.
Covino, S., Panzera, M. R., Tagliaferri, G., & Pallavicini, R. 2001, A&A, 371, 973
Donati, J.-F. 1999, MNRAS, 302, 457
Donati, J.-F., Collier Cameron, A., Semel, M., et al. 2003, MNRAS, 345, 1145
Fekel, F. C., Bopp, B. W., Africano, J. L., et al. 1986a, AJ, 92, 1150
Fekel, F. C., Moffett, T. J., & Henry, G. W. 1986b, ApJS, 60, 551
Frasca, A., Biazzo, K., Kővári, Zs., et al. 2010, A&A, 518, A48
Frasca, A., Biazzo, K., Taş, G., Evren, S., & Lanzafame, A. G. 2008a, A&A, 479, 557
Frasca, A., Kővári, Zs., Strassmeier, K. G., & Biazzo, K. 2008b, A&A, 481, 229
Gálvez, M. C., Montes, D., Fernández-Figueroa, M. J., De Castro, E., & Cornide, M. 2009, AJ, 137, 3965
García-Alvarez, D., Foing, B. H., Montes, D., et al. 2003, A&A, 397, 285
Gu, S.-h., Tan, H.-s., Shan, H.-g., & Zhang, F.-h. 2002, A&A, 388, 889
Gunn, A. G., & Doyle, J. G. 1997, A&A, 318, 60
Gunn, A. G., Doyle, J. G., & Houdebine, E. R. 1997, A&A, 319, 211
Hall, J. C., & Ramsey, L. W. 1992, AJ, 104, 1942
Huenemoerder, D. P. 1986, AJ, 92, 673

Jetsu, L. 1993, A&A, 276, 345
Kővári, Zs., Strassmeier, K. G., Granzer, T., et al. 2004, A&A, 417, 1047
Landman, D. A., & Mongillo, M. 1979, ApJ, 230, 581
Lehtinen, J., Jetsu, L., Hackman, T., Kajatkari, P., & Henry, G. W. 2012, A&A, 542, A38
López-Santiago, J., Montes, D., Fernández-Figueroa, M. J., & Ramsey, L. W. 2003, A&A, 411, 489
Montes, D., Fernández-Figueroa, M. J., De Castro, E., & Cornide, M. 1995, A&A, 294, 165
Montes, D., Fernández-Figueroa, M. J., De Castro, E., & Sanz-Forcada, J. 1997, A&AS, 125, 263
Montes, D., Fernández-Figueroa, M. J., De Castro, E., et al. 2000, A&AS, 146, 103
Montes, D., Saar, S. H., Collier Cameron, A., & Unruh, Y. C. 1999, MNRAS, 305, 45
Rice, J. B., & Strassmeier, K. G. 1998, A&A, 336, 972
Shine, R. A., & Linsky, J. L. 1972, SoPh, 25, 357
Shine, R. A., & Linsky, J. L. 1974, SoPh, 39, 49
Strassmeier, K. G., Fekel, F. C., Bopp, B. W., Dempsey, R. C., & Henry, G. W. 1990, ApJS, 72, 191
Strassmeier, K. G., Rice, J. B., Wehlau, W. H., Hill, G. M., & Matthews, J. M. 1993, A&A, 268, 671
Vilhu, O., Gustafsson, B., & Walter, F. M. 1991, A&A, 241, 167
Zhang, L.-Y., & Gu, S.-H. 2008, A&A, 487, 709
Zirin, H. 1988, Astrophysics of the Sun (Cambridge: Cambridge Univ. Press)